Original Article
Sevoflurane prevents pulmonary vascular remodeling and right ventricular dysfunction in pulmonary arterial hypertension in rats

Wenqian Zhai[1*], Yunfei Li[1*], Yongjuan Luo[2], Weidong Gao[3], Shan Liu[4], Jiange Han[1], Jie Geng[5]

Departments of [1]Anesthesiology, [2]Ultrasonics, [5]Cardiology, Tianjin Chest Hospital, Tianjin 300222, China; [3]Department of Anesthesiology & Critical Care Medicine, Johns Hopkins University School of Medicine, Baltimore 21205, MD, USA; [4]Tianjin Cardiovascular Institute, Tianjin Chest Hospital, Tianjin 300051, China. *Equal contributors.

Abstract: Background: The cardioprotective properties of sevoflurane have been reported in studies of the left ventricle. However, whether this volatile anesthetic would also be beneficial for pulmonary vascular remodeling and associated right ventricular hypertrophy (RVH) remained to be explored. Here, we investigated the potential benefit of sevoflurane to right heart function in experimental pulmonary arterial hypertension (PAH). Methods: Adult Wistar rats received one dose peritoneal injection of monocrotaline (MCT, 60 mg/kg) or the equal volume of normal saline. Two weeks later, rats were treated with sevoflurane or sham exposure. PAH status and cardiac function were assessed by echocardiography weekly, and the body weight (BW) was monitored every week. After 6 weeks of exercise, Fulton's index calculation, histological observation, IL-6 and TNF-α immunohistochemical analyses, evaluation of MDA, SOD and GSH-Px levels and NF-κB and MAPK active determination were performed in lung and RV tissue samples. Results: MCT induced pulmonary vascular remodeling, RVH, increased Fulton's index ($P<0.01$), and right ventricular failure (RVF) in rats. Animals inhaled sevoflurane had an increased cardiac output ($P<0.05$) and lower incidence of RVF ($P<0.05$). Also, these animals had a reduced RVEDD, RVWTd and PAID ($P<0.05$), increased PV ($P<0.05$), reduced wall thickness and vascular wall area of pulmonary small vascular (vascular external diameter 50-150 um) ($P<0.01$), reduced RV fibrosis, and increased RV cardiomyocyte area ($P<0.01$). Furthermore, sevoflurane reduced IL-6 and TNF-α expression in lungs and heart ($P<0.01$), decreased level of MDA ($P<0.01$) and increased activity of SOD and GSH-Px ($P<0.01$). In addition, it decreased the activities of NF-κB and MAPK pathways ($P<0.01$). Conclusion: Sevoflurane reduces pulmonary vascular remodeling and RVH in PAH induced by MCT in rats. This effect is likely due to down-regulation of inflammatory factors IL-6 and TNF-α, reduced level of oxidative stress and the inhibition of NF-κB and MAPK pathways.

Keywords: Pulmonary arterial hypertension (PAH), right ventricular hypertrophy (RVH), right ventricular failure (RVF), sevoflurane

Introduction

Pulmonary arterial hypertension (PAH) is a life-threatening disease characterized by progressive pulmonary vasoconstriction leading to pulmonary vascular remodeling, and causes the right heart hypertrophy leading to right ventricular failure (RVF) eventually. Although the pathophysiology of PAH has been increasingly recognized, its mortality remains high when RVF develops.

Cardioprotective properties of volatile anesthetics, represented by sevoflurane, have been recognized in preclinical and clinical studies. Sevoflurane administrated before and during ischemia-reperfusion (IR) injury in isolated rat hearts improved the recovery of left ventricle (LV) work, an index of IR injury [1]. This finding is consistent with observation from animal models of LV IR injury *in vivo*, even if the drug was inhaled for only a short duration before ischemia [2]. Moreover, translational clinical studies suggest that there is a reduction in myocardial damage and mortality in patients treated with sevoflurane during cardiac surgery [3-5]. Furthermore, two international consensus con-

ferences had indicated that the administration of volatile anesthetics is one of the important nonsurgical interventions that is associated with survival benefit [6, 7]. Despite the findings that cardioprotective properties of inhaled anesthetics have been reported in the left heart, there has been little scientific evidence on the beneficial effects of sevoflurane in the right heart.

Inflammation, or more specifically, altered immune process and failure to resolve inflammation, is a compelling signal that causes poor prognosis in PAH patients [8]. Growing studies consistently show that targeting the inflammation could be a potential method to assess and treat right ventricular hypertrophy (RVH) and pulmonary arterial remodeling. Many common signaling molecules, such as NF-κB, MMP-9, TNF-α, IL-6, IL-1, HMGB1, and NLRP3, initiate inflammation response to cause injury. Sevoflurane has been shown to possess anti-inflammation functions. A study described a novel approach to using sevoflurane as a local anti-inflammatory drug, not as an anesthetic, to attenuate inflammatory response both locally and systemically through intramyocardial delivery of sevoflurane in patients undergoing elective mitral valve surgery [9]. Hypothetically, sevoflurane can also prevent pulmonary vascular remodeling and RVH via its anti-inflammation function.

Here, we aimed to investigate the contribution of sevoflurane to pulmonary vascular remodeling and right ventricle (RV) dysfunction in rat model of PAH. In addition, we determined if NF-κB and MAPK pathways are involved in this effect.

Methods

MCT rat model of PAH

The study was approved by the Ethics Committee of Animal Research of Tianjin Medical University (permission number SYXK(Jin): 2019-0004). Forty-eight clean-grade healthy male adult Wistar rats (Charles River Lab, China), weighting 250-280 g, were used. All animals were raised in constant temperature and humidity with regular light-dark cycle, and had standard chow and tap water ad libitum. One week later, rats were randomly assigned into four groups: Control (group C, n=12), con-

trol + sevoflurane group (group CS, n=12), monocrotaline (MCT) group (group M, n=12), and MCT + sevoflurane group (group MS, n=12). In group M and group MS, PAH was induced by an intraperitoneal injection of MCT (CrotalineC2401, 60 mg/kg, Sigma-Aldrich, Buchs, Switzerland), and equal volume of normal saline was injected at the same time in group C and group CS. Diet and activity were monitored closely during the entire course of the experiment for all rats, with the body weight (BW) obtained weekly. All animal care and procedures followed the institutional guideline.

Administration of sevoflurane

The rats in group CS and group MS were placed in a sealed resin box and inhaled 1.5 MAC sevoflurane (Abbott, Baar, Switzerland) (mixed with 100% oxygen) input through air inlet using an anesthetic gas evaporator. The concentration of sevoflurane in the box was monitored continuously using a concentration monitor (Ultima™, Datex/Instrumentarium, Helsinki, Finland), which was connected to air outlet. One hour later, the animal was recovered. Sevoflurane was administered twice a week until 6 weeks for two weeks after MCT injection and the animals in other groups were put in the same environment but did not inhale sevoflurane.

Echocardiography

PAH status and cardiac function were confirmed by echocardiography weekly. Before the examination was performed, all rats including control group were anesthetized using 2.5% isoflurane (2:1 ratio of isoflurane: O_2). Three electrodes were placed on the three limbs of rats for electrocardiogram variability analysis. Echocardiography was performed using an ultrasound transducer (Philips Ultrasound, Inc., L15-7io, USA), according to previously described methods [10]. After the chest was shaved, the LV end-systolic and end-diastolic volumes were measured from M-mode images (two dimensional) which were obtained from a short axis LV view at the level of the papillary muscles. Then, LV cardiac output (equal to RV cardiac output) was calculated. Cardiac output (ml) = (end-diastolic volume-end systolic volume) × heart rates. The RV end-diastolic dimension (RVEDD), RV wall thickness in diastole (RVWTd), intraventricular septum in diastole (IVSd), and

LV posterior wall thickness in diastole (LVPWd) were measured from the parasternal long axis LV view. The maximal velocity of pulmonic valve (PV) and pulmonary arterial internal dimension (PAID) were measured from pulmonic valve flow pulse wave Doppler signal obtained at the parasternal short axis LV view. All echocardiographic examinations were performed by the same person at heart rates from 350 to 400 beats/min under anesthesia.

Evaluation of right ventricular hypertrophy

After sacrifice of the rats, the thoraxes were opened and the hearts were dissected with atria removed before separating RV from the LV and septum. The weight of these two parts was determined by reassembling the respective slices to obtain Fulton's index (the ratio of RV/LV+S).

Histological analysis of lungs and heart

The lungs (the upper lobe of the right lung) and hearts were fixed in 10% formalin (pH 7.4) for 24 hours, embedded with paraffin, sliced serially (4 um), and strained with HE and Masson Trichrome. Histologic images of lungs and hearts tissues, including pulmonary small vessels, were captured with an optical microscope and analyzed using image pro plus 6.0. The external diameter (ED), internal diameter (ID), total vascular area (TA), lumen area (LA), wall thickness (WT), wall area (WA), WT% ((ED-ID)/ED × 100%), WA% ((TA-LA)/TA × 100%) of the pulmonary arterioles and the cardiomyocyte cross-sectional area were calculated. Cardiomyocyte cross-sectional area was obtained from cells with nucleuses located in the center of the histologic images. In addition, cardiac fibrosis was evaluated from Masson Trichrome by assessing the blue pixels.

Immunohistochemstry of lungs and heart

Paraffin sections of lungs and heart specimens (each thickness is 4 µm) were dewaxed in 100% toluene twice, and then rehydrated by immersing in decreasing ethanol concentration (100%, 95%, 85%, 75%) and in distilled water finally. Endogenous peroxidase activity was blocked with 0.3% (vol/vol) H_2O_2 in methanol for 15 minutes. After three washes with PBS, the sections were then preincubated in 3% (vol/vol) bovine serum albumin in PBS for 30 min, and incubat-ed with polyclonal anti-IL-6 (Bioss Cat# bs-0782R-Biotin, RRID: AB_11085421) or anti-TNF-α (1:100 in PBS, Bioss, China) antibodies overnight at 4°C. The sections were then washed three times with PBS, exposed to biotin-labeled secondary antibodies (Dako, Trappes, France) for 1 hour and then in 3,3'-diamino-benzidine tetrahydrochloride dihydrate (DAB, Sigma, St Louis, MO) for peroxidase straining. Finally, the sections were exposed to hematoxylin for several seconds. After viewed and photographed under an optical microscope, Image Pro Plus 6.0 software was used to select the brownish yellow areas of the immunohistochemical complex in the image, and the average optical density value (IOD) of these areas was measured.

Measurement of oxidative stress levels

After tissue homogenization, commercial oxidative stress kits (Nanjing Jiancheng Bioendineering Institute, China) were used to respectively detect the level of MDA and activity of SOD and GSH-Px in the upper lobe of the right lung and RV tissues.

Western blot assay

Total protein was separated from the upper lobe of the right lung and RV tissues using the protein extraction kit (Bio-Rad, USA) and the protein concentration was determined using the BCA protein quantitative kit (Beyotime, China). After resolved using SDS-PAGE, protein samples (20-50 µg) were moved to polyvinylidene fluoride (PVDF) membrane (Millipore, USA) and probed with antibodies against p-P65 (Cell Signaling Technology Cat# 3037, RRID: AB_2341216), P65 (Cell Signaling Technology Cat# 3034, RRID:AB_330561), pIκBα (Cell Signaling Technology, USA, 1:1000), IκBα (Cell Signaling Technology Cat# 8993, RRID: AB_2797687), pERK1/2 (Cell Signaling Technology Cat# 9101, RRID:AB_331646), ERK1/2 (Cell Signaling Technology Cat# 9102, RRID: AB_330744), p-P38MAPK (Cell Signaling Technology Cat# 5302, RRID:AB_561213), P38-MAPK (Cell Signaling Technology Cat# 9217, RRID:AB_331298), GAPDH (Proteintech, USA, 1:5000), Tubulin (Proteintech, USA, 1:5000), and β-actin (Proteintech, USA, 1:5000), followed by appropriate secondary antibody. All Western blots were repeated at least three times.
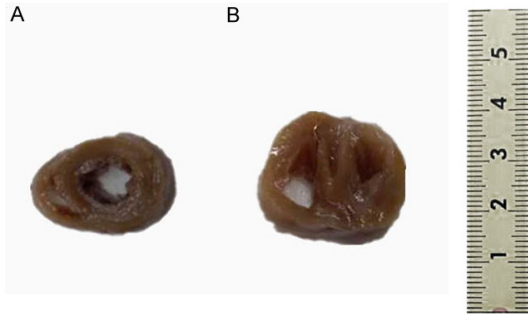
Figure 1. Representative midinterventricular septum transverse sections of hearts from group C (A) and group M (B).

Table 1. Heart weight of rats in all groups

Parameters	Group C	Group M
Heart weight (mg)	1034±171	1189±150
Left ventricular weight (mg)	878±144	899±153
Right ventricular weight (mg)	141±36	201±51*
Fulton's index (%)	30.1±8.1	41.3±7.3**

All values are presented as mean ± SD. Group C, n=12; Group M, n=12. *$P<0.05$ and **$P<0.01$ compared with corresponding values in Group C.

Statistical analysis

Statistical analyses were performed with SPSS 23.0. Dates are reported as mean ± SD. *P* values of <0.05 or <0.01 were considered significant. Normality of date was checked, and either log-transformation or nonparametric testing was performed if data were not normally distributed. The effects of MCT injection compared with control group and the effects of sevoflurane compared with MCT were characterized by Student's t-test. The effects of sevoflurane compared with MCT and control were characterized by a one-way repeated measure ANOVA. The percent RVF between group M and group MS was performed by Kaplan-Meier analysis.

Results

PAH induced by MCT injection in right heart

At the end of the study, i.e., 6 weeks after MCT injection (or 1-2 weeks earlier), most rats in group M presented various clinical signs of RVF such as dyspnea, wheezing, cyanosis of the nose and lips, lethargy, decreased activity, reduced food intake, and erect hair. Some rats in this group also had pericardial and pleural effusions. **Figure 1** shows the histologic changes in the hearts of animals from group C and group M. The RV wall was thickened with dilatation. There were no significant differences in the mean heart weight (1034±171 g *vs.* 1189±150 g, *P>0.05*) and LV weight (878±144 g *vs.* 899±153 g, *P>0.05*) between the two groups, but the mean RV weight in group M was statistically more than that in group C (201± 51 g *vs.* 141±36 g, *P<0.05*) (**Table 1**). Fulton's index between the two groups was also significantly different (41.3±7.3 *vs.* 30.1±8.1, *P<0.05*) (**Table 1**). Clearly, RVF developed as a result of MCT injection.

Sevoflurane improved right heart function and prevented progression toward RVF

To investigate whether sevoflurane administration impacts the development of RVF, we administrated sevoflurane via inhalation intermittently for 1 hour twice a week for two weeks after MCT injection and performed serial echocardiography to follow changes in the right heart. We calculated cardiac output to evaluate heart systolic function at the end of experiment. As is shown in **Figure 2A**, cardiac output was significantly different in group MS in comparison with Group M (70.65±1.33 ml/min *vs.* 52.35±1.65 ml/min, *P<0.05*). In addition, survival analysis indicated that sevoflurane could prevent the progression toward RVF in comparison with animals only injected with MCT (**Figure 2B**, *P<0.05*).

Figure 2C shows the weekly changes in mean BW (ΔBW) 1, 2, 3, 4, 5 and 6 weeks after MCT injection, and **Figure 2D** shows the overall changes in BW after the final recordings (ΔBW6) in four groups. The weight of control group and group CS maintained steady growth, whereas in MCT group the weight reduced at week 6 (**Figure 2C**). MCT injection was associated with a relatively reduced ΔBW6 (89.75± 6.86 g *vs.* 150.87±14.64 g, *P<0.05*) and animals that inhaled sevoflurane (at MAC 1.5) presented an increased ΔBW6 (113.83±11.53 g *vs.* 89.75±6.86 g, *P<0.05*) (**Figure 2D**).

These data show that sevoflurane can protect right heart from pathologic remodeling, maintain right heart function, and prevent the progression towards RVF during pulmonary hypertension.
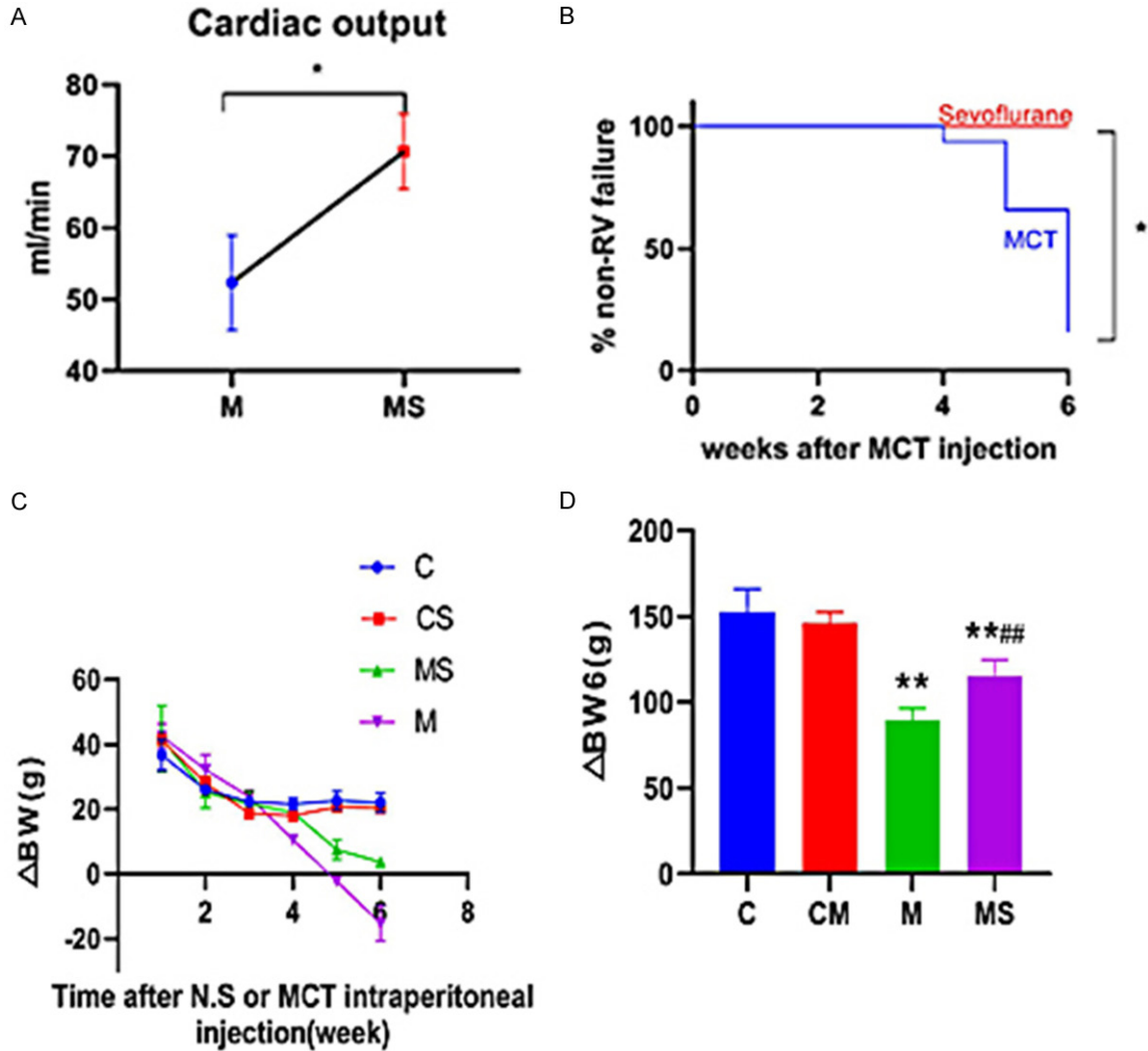
Figure 2. Sevoflurane improved right heart function and prevented progression toward RVF. Sevoflurane administration improved cardiac output (A, *$P<0.05$ compared with corresponding values in Group M) and delayed time to right heart failure (B, *$P<0.05$ compared with corresponding values in Group M) and increased body weight (C and D, **$P<0.01$ compared with corresponding values in Group C. ##$P<0.01$ compared with corresponding values in Group M).

Sevoflurane reduced pulmonary vascular remodeling and RVH

Echocardiography was performed to determine the structure changes in the RV. **Figure 3** shows the echocardiography images of three representative rats from each group. **Figure 3A** shows the parasternal long axis LV view and it was observed that RV was obviously enlarged, the RV wall was thickened, and the interventricular septum expanded to LV, resulting in compression of the left ventricular cavity. **Figure 3B** is pulmonic valve flow pulse wave Doppler signal obtained at the parasternal short axis LV view, and the blood flow spectrum of pulmonary arteries in group M showed an asymmetrical inverted triangle, even daggers, with a reduced peak and a significant forward shift. **Figure 3C** represents pulmonary vascular diameter measurements at the parasternal short axis LV view (long axis pulmonary artery section), and widening and dilation of the RV outflow tract and pulmonary artery were observed. The parameters obtained from echocardiography are presented in **Table 2**. At MAC 1.5, sevoflurane decreased RVEDD (0.263± 0.013 mm *vs.* 0.331±0.015 mm, $P<0.05$), RVWTd (0.217±0.006 mm *vs.* 0.254±0.011 mm, $P<0.05$) and PAID (0.333 and P *vs.* 0.355±0.009 mm, $P<0.01$), but increased PV

Sevoflurane prevents pulmonary arterial hypertension

A   B   C

Group C

Group CS

Group M

Group MS
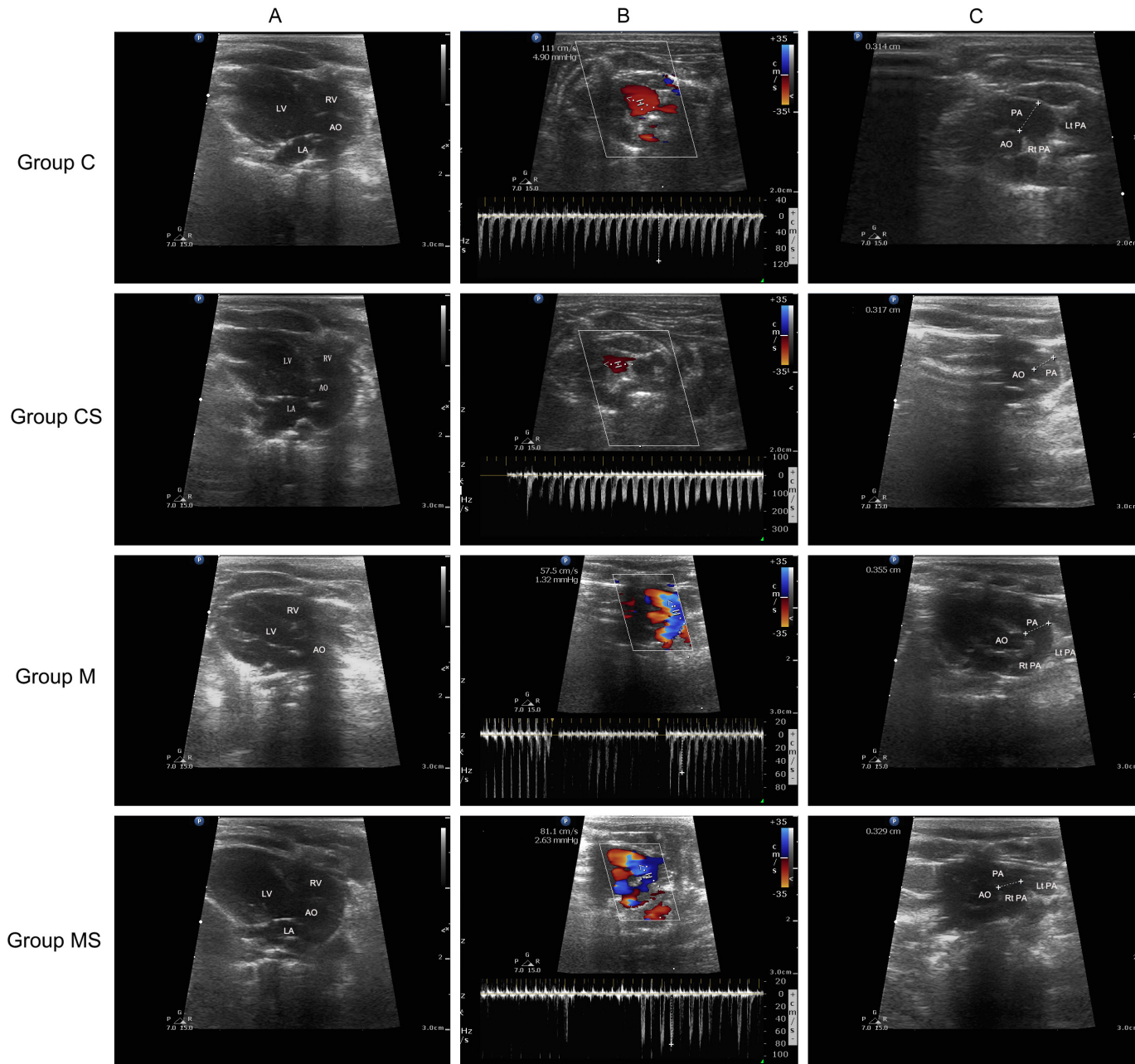
Figure 3. Representative echocardiographic tests graph. A. The parasternal long axis LV view; B. Pulmonic valve flow pulse wave Doppler signal obtained at the parasternal short axis LV view; C. Pulmonary vascular diameter measurements at the parasternal short axis LV view (long axis pulmonary artery section). LA, left atrium; AO, the aorta; PA, pulmonary artery; Rt PA, right pulmonary artery; Lt PA, left pulmonary artery.

Table 2. The recordings of echocardiography

Variable	Group C	Group CS	Group M	Group MS
RVEDD (mm)	0.213±0.009	0.221±0.011	0.331±0.015*	0.263±0.013*,#
RVWTd (mm)	0.116±0.106	0.130±0.017	0.254±0.011*	0.217±0.006*,#
IVSd (mm)	0.133±0.006	0.139±0.013	0.175±0.021*	0.162±0.009*
LVPWd (mm)	0.132±0.003	0.145±0.016	0.162±0.022	0.160±0.007
PV (m/s)	106.633±2.542	103.301±2.457	57.353±5.379*	80.538±5.446*,#
PAID (cm)	0.312±0.002	0.314±0.003	0.355±0.009**	0.333±0.004**,##

All values are presented as mean ± SD. Group C, n=12; Group CS, n=12; Group M, n=12; Group MS, n=12. *$P<0.05$ compared with corresponding values in Group C. **$P<0.01$ compared with corresponding values in Group C. #$P<0.05$ compared with corresponding values in Group M. ##$P<0.01$ compared with corresponding values in Group M. RVEDD: the right ventricle end-diastolic dimension; RVWTd: right ventricle wall thickness in diastole; IVSd: intraventricular septum in diastole; LVPWd: LV posterior wall thickness in diastole; PV: the maximal velocity of pulmonic valve; PAID: pulmonary arterial internal dimension.

(80.538±5.446 *vs.* 57.353±5.379 cm/s, $P<0.05$).

To gain more insight into the pulmonary artery and RV remodeling at cellular level, HE staining of tissue sections from the lungs and hearts was performed (**Figure 4A**, **4B**). Compared to control group, the group M had small pulmonary vessel intimal hyperplasia and luminal narrowing along with congestion and structure disorder (**Figure 4A**, **4C-E**, $P<0.01$), which conform to pulmonary hypertensive changes. However, sevoflurane inhalation decreased media and intima wall thickness of pulmonary small vessel (**Figure 4A**, **4C-E**, $P<0.01$). In group M, the area of cardiomyocyte was increased (**Figure 4B**, **4F**, 240.179±29.185 *vs.* 64.843±18.896, $P<0.01$), consistent with RVH. Sevoflurane reduced RV cardiomyocyte area (**Figure 4B**, **4F**, 150.659±28.253 μm^2 × 10^4 *vs.* 240.179±29.185 um^2 × 10^4, $P<0.01$). Furthermore, we examined the content of collagen fiber by masson staining and found that sevoflurane also decreased the amount of fibrosis, an important pathophysiological feature of RVH as compared to M group (**Figure 4G**). These data show that sevoflurane protected right heart from pathological remodeling and failing during PAH.

Sevoflurane reduced pulmonary and cardiac inflammation

To assess whether the improved RV function, reduced pulmonary vascular and RV remodel-

ing by sevoflurane are related to inhibition of inflammation, we performed immunohistochemical analysis of inflammatory factors IL-6 and TNF-α in tissues of lungs and hearts. Since there were no significant differences in the degree of pulmonary vascular remodeling, RV structure and function between group C and CS, we selected rat samples from group C, group M and group MS for subsequent experiments (**Figure 5**). Exposure to MCT was associated with a rapid rise in lung IL-6 (**Figure 5A**, 517.359±63.831 *vs.* 77.715±20.288, $P<0.01$) and TNF-α (**Figure 5B**, 567.349±80.223 *vs.* 70.535±24.267, $P<0.01$) immunostaining. Cardiac tissue IL-6 (**Figure 5C**, 896.803±170.864 *vs.* 74.179±58.081, $P<0.01$) and TNF-α (**Figure 5D**, 646.803±83.226 *vs.* 96.322±53.953, $P<0.01$) levels were also increased in week 6. In contrast, levels of IL-6 and TNF-α in both lungs (IL-6, **Figure 5A**, 377.410±69.829 *vs.* 517.359±63.831, $P<0.01$; TNF-α, **Figure 5B**, 477.460±40.387 *vs.* 567.349±80.223, $P<0.01$) and hearts (IL-6, **Figure 5C**, 488.047±86.792 *vs.* 896.803±170.864, $P<0.01$; TNF-α, **Figure 5D**, 421.381±72.452 *vs.* 646.803±83.226, $P<0.01$) were significantly lower in rats treated with sevoflurane. These findings suggest that sevoflurane produced anti-inflammation and anti-oxidative stress effects and maintained RV function, thus preventing the development of RVF during PAH.
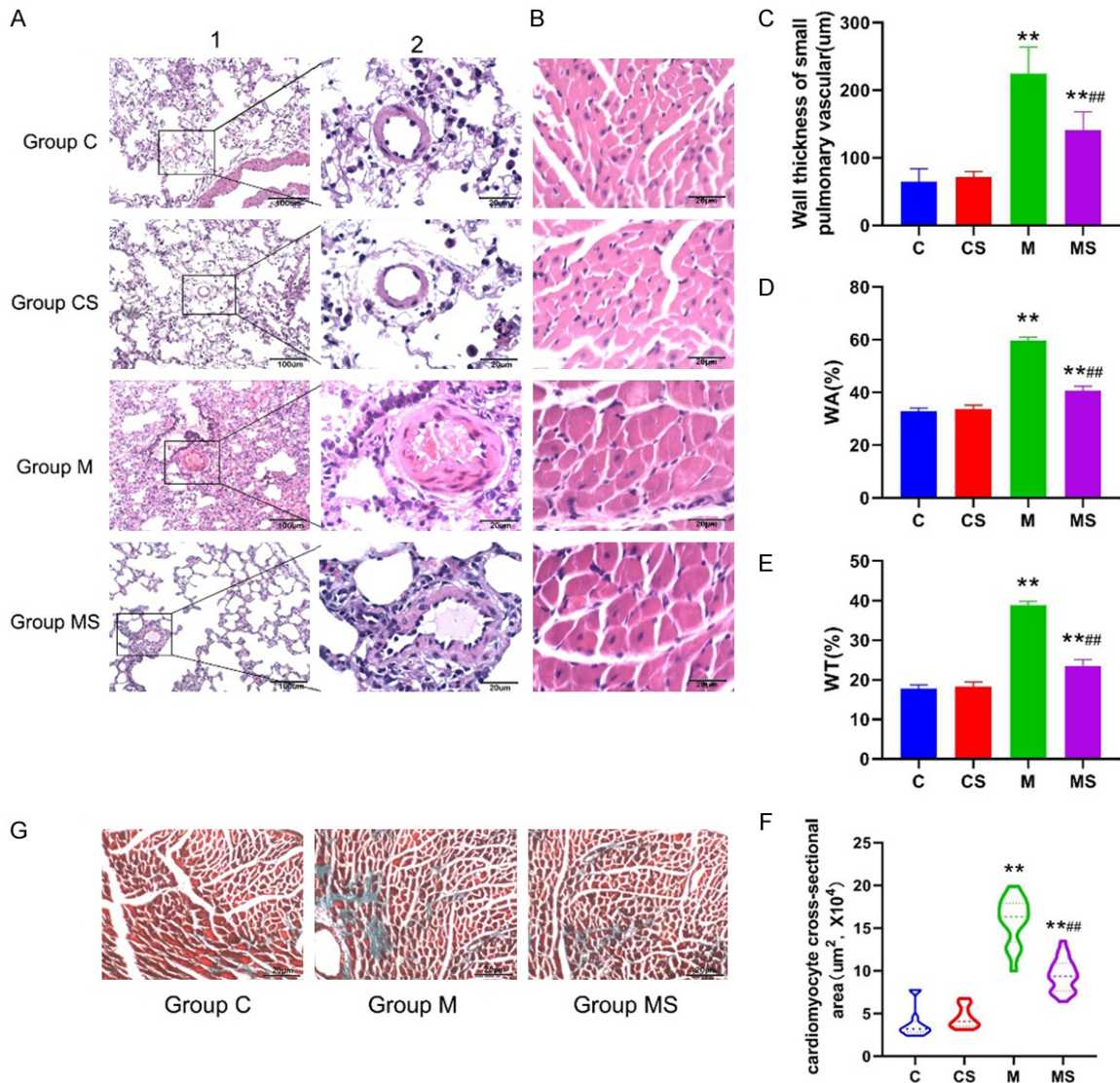
Figure 4. Morphologic images of lungs and heart sections from rats. Lungs section from the right upper lobe with small vessel intimal hyperplasia and luminal narrowing, along with congestion and structure disorder (A1, HE, original magnification 100). Small pulmonary vessel intimal proliferation and luminal narrowing (A2, HE, original magnification 400). HE staining of heart section from RV of rats with cardiomyocyte area increased (B, HE, original magnification 400). Identification of collagenous fiber of heart tissue by masson staining (G, original magnification 100). The thicknesses of the pulmonary small vascular and the areas of myocardial cells are semiquantitative analyzed and visible (C-F). **$P<0.01$ compared with corresponding values in Group C; ##$P<0.01$ compared with corresponding values in Group M.

Sevoflurane inhibition NF-κB and MAPK pathways

As is shown in **Figure 6**, p-P65/P65, pIκBα/IκBα, pERK1/2/ERK1/2 and p-P38MAPK/P38MAPK expression levels were significantly higher in group M than those in group C ($P<0.01$), but were significantly lower in the MS group than those in the M group ($P<0.01$), indicating that NF-κB and MAPK pathways were

involved in sevoflurane's protective effect on pulmonary vascular remodeling and RV dysfunction in PAH in Rats.

Discussion

RV function in pulmonary hypertension and the model of PAH

In the recent years, the importance of RV has been widely recognized, but it still remains
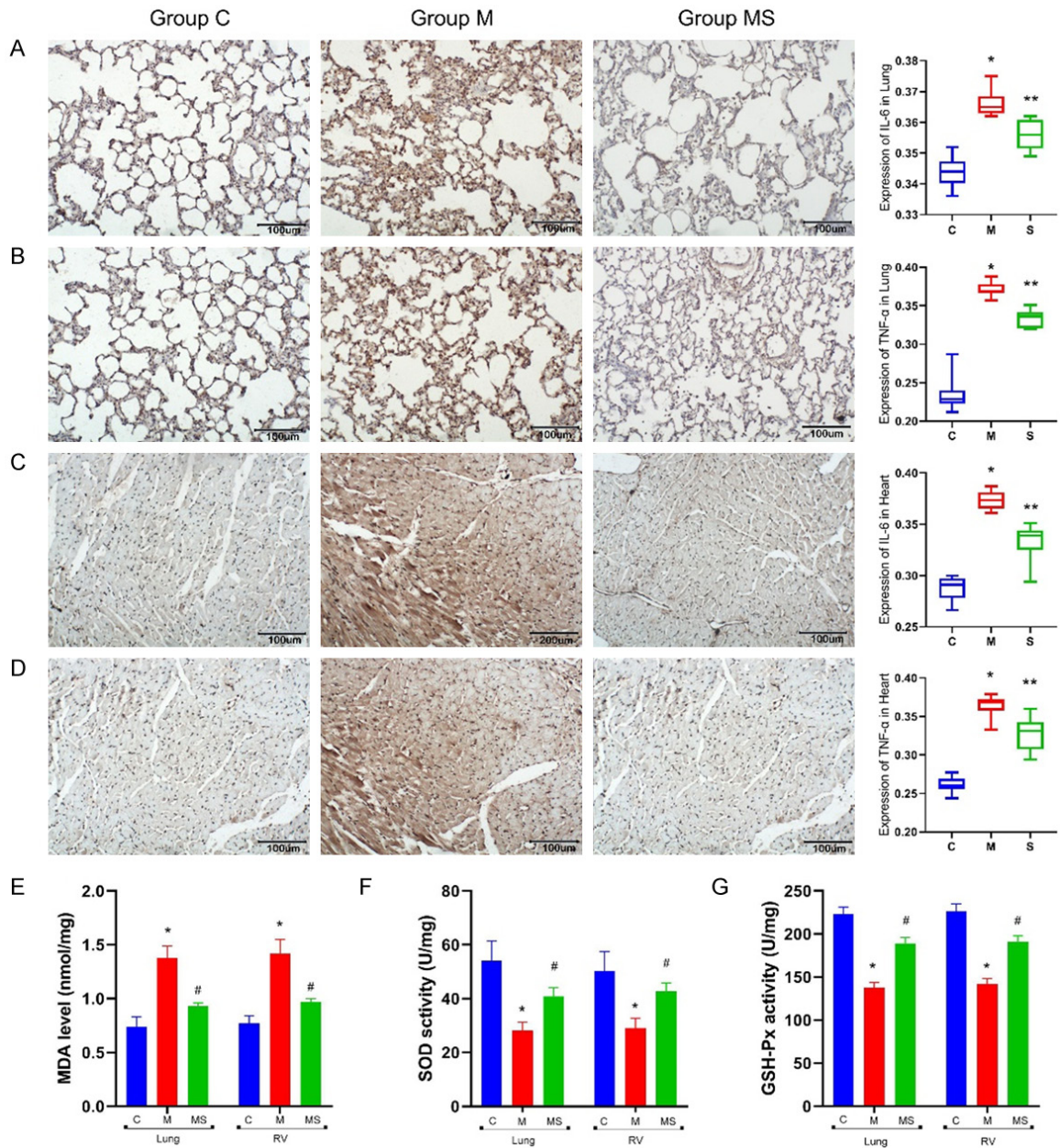
Figure 5. Immunolocalization of interleukin-6 (IL-6) and tumor necrosis factor-α (TNF-α) and oxidative stress levels (E-G) in lungs and heart from rats (original magnification 100). IL-6 levels (A) and TNF-α levels (B) in lung tissue, IL-6 (C) and TNF-α (D) levels in cardiac tissue. MDA level (E), SOD (F) and GSH-Px (G) activity in lung and cardiac tissue. Each value is semiquantitatively analyzed. *$P<0.05$ compared with corresponding values in Group C; #$P<0.05$ compared with corresponding values in Group M.

understudied compared with the LV. There are many differences between RV and LV, so knowledge from the LV cannot be directly applied to the RV. In pulmonary hypertension, RV adapts to the increasing afterload by enhancing contractility to maintain the blood flow. The gradual dysfunction and failure of the RV remained as the main contributors to mortality and disability for patients with pulmonary hypertension. Moreover, RV dysfunction is a better important independent risk factor for predicting the prognosis of patients than pulmonary vascular resistance. A multicenter clinical study showed that RVF accounts for 70% cause of the death in patients with PAH [11]. Taken together, it is crucial to pay attention to and protect the RV function of patients in the perioperative period.
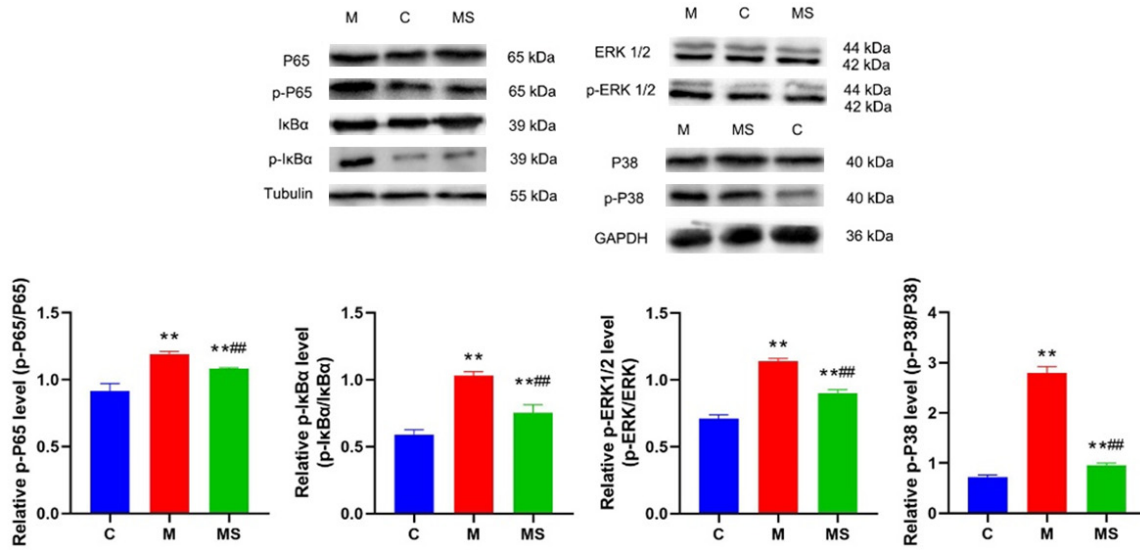
Figure 6. The relative protein level of p-P65, P65, pIκBα, IκBα, pERK1/2, ERK1/2, p-P38MAPK, P38MAPK, GAPDH, Tubulin and β-actin in RV tissues of rats detected by WB. $^{**}P<0.01$ compared with corresponding values in Group C; $^{##}P<0.01$ compared with corresponding values in Group M.

We elected MCT 60 mg/kg to be injected intraperitoneally to establish the model of pulmonary vascular remodeling and RVH. MCT is a toxic pyrrolizidine alkaloid found in the plant Crotalaria spectabilis, which can cause acute and subacute damages of the peripheral vasculature of lung through early adventitial inflammation followed by progressive smooth muscle hypertrophy in the media [12]. In the present study, after MCT injection, RV wall thickness and weight were both increased (**Figures 1**, **3**; **Tables 1**, **2**) and cardiac output was decreased (**Figure 2A**). These results confirmed that the RV adapted to the increased pulmonary arterial pressure through concentric hypertrophy, however, because RV systolic function measured by cardiac output was still impaired, this adaptation can be considered as insufficient and final result in RVF (**Figure 2B**).

Inflammation, pulmonary vascular remodeling and RVH

Previous studies have demonstrated the important role of inflammation in pathogenesis of PAH, and the involvement of IL-6 and THF-α in the inflammation pathway has been described. In animal model of hypoxic pulmonary hypertension, levels of 48 mRNAs associated with inflammation were upregulated [13]. Bone morphogenetic protein receptor 2 (BMRP2) [14], NF-κB [15], transforming growth factor

beta (TGF-β) signaling pathways changes had also been linked to rat or mice models of PAH and had interrelation with each other. Using IL-6$^{-/-}$ mice, Laurent Savale et al. [16] found that the numbers of muscular pulmonary vessels and inflammation cells recruitment were reduced after 2 weeks of hypoxic treatment than in IL-6$^{+/+}$ mice, suggesting the specific role of IL-6 in attenuating the development of PAH in mice. In addition, increased levels of proinflammatory factors like IL-6, Tnf, Ccl-2 have been reported in PAH patients [17, 18]. Furthermore, these elevated levels of inflammation cytokines could predict survival in patients with PAH [19], and were even superior to traditional prognostic markers, such as 6-minute walking and hemodynamics. In human RVF, inflammatory pathway had been demonstrated to be more important in RV tissue [20]. Circulating dendritic cells as well as tissue resident immune cells could reflect right heart function [21]. More importantly, inflammation was even involved in PAH with left heart failure [22]. In the present study, we provided direct evidence that local inflammation activity of the lungs and heart in experimental PAH is significant (**Figures 4A**, **5**). In addition, we demonstrated that reduced inflammation is associated with reduced pulmonary vascular remodeling and RVH. These findings suggest a crucial pathophysiological role of inflammation in PAH.

The effects of sevoflurane

Previous studies in animal models of IR injury have described the beneficial effects of sevoflurane and inflammation response in this process. However, the anti-inflammation action of sevoflurane in experimental PAH is still unknown. In the current study, we offer evidence that sevoflurane inhaled at MAC 1.5 reduced lungs and heart local proinflammatory markers IL-6 and TNF-α production (**Figure 5**), resulting in protection of the RV during PAH, and this effect may be associated with NF-κB and MAPK pathways (**Figure 6**). Sevoflurane administration was associated with decreased small vessel intimal hyperplasia and luminal narrowing, along with less congestion and structure alterations, as observed in HE straining (**Figure 4A**).

The concentration of the inhalation anesthetic used is discrepant in different studies. It can be adjusted to the animal's response to deep paw pinch (animals were further hyperventilated to avoid spontaneous breathing during recordings) or obey strictly imposed MAC as in the present study. However, different experimental protocol may influence the underlying sympathetic tone between studies, a consequence that is in connection with cardiovascular changes in PAH. In previous studies on sevoflurane pretreatment or postconditioning in myocardial IR injury either *in vitro* or *in vivo*, researchers have demonstrated that 2.4-3.6 vol% (equal to 1-1.5 MAC) sevoflurane [23-26] could produce anti-ischemia effects. Also, in the preliminary experiment, we had confirmed that sevoflurane at 1.5 MAC would not prevent the occurrence of spontaneous breathing of rats, and this is consistent with the clinical effective dose of sevoflurane [27].

Inflammation is considered to be a crucial mediator of complications of cardiac surgery. And sevoflurane has been proved to have the ability to quench inflammation. Previous studies have demonstrated reduced plasma or alveolar levels of TNF-α, IL-1β, IL-6, IL-8, and INF-γ and increased levels of IL-10 in animal models of lung injury from various causes [28-31] and patients with acute respiratory distress syndrome (ARDS) [32] when administrated with sevoflurane. Other preclinical studies, such as spinal cord IR, murine allergic airway inflamma-

tion, also confirm this potential of sevoflurane on pro-inflammation and anti-inflammation factors. Of interest, new applications of sevoflurane have been tried in cardiac surgery and allergic airway inflammation to achieve better anti-inflammation effect, such as intramyocardial delivery, repeated inhalation. More importantly, even sevoflurane metabolite hexafluoro-2-propanol also has a potential of immunomodulatory effect by reducing IL-6 expression in a rat model of endotoxaemia. The level of these cytokines is closely related to the prognosis of patients. And the anti-inflammation effect of sevoflurane is mainly regulated via inhibition of the NF-κB, TLR4, NLRP3, or other signaling pathway.

The physiological function of NF-κB has been widely studied. It can regulate the expression of various growth factors (such as VEGF), inhibit the apoptosis of PASMCs, regulate the expression of IL-6 and other inflammatory factors, and interfere with immune regulation, making it a research hotspot in the pathophysiological mechanism of pulmonary vascular remodeling in PAH. The activation of NF-κB was found in the lung tissue of PAH patients and in the animal PAH models induced by SU5416, chronic hypoxia and MCT, and was found throughout the whole PAH disease process. In the present study, MCT treatment induced up-regulation of p-P65 and pIκBα, indicating the involvement of NF-κB in PAH and RVH, and sevoflurane could regulate the expression of key NF-κB protein to reduce the pathological changes of RV (**Figure 6**). Notably, inhibition of NF-κB did not reduce IL-6 levels in PAH lung tissue, suggesting that there are other signaling pathways or molecules that stimulate IL-6 secretion in advanced PAH [33].

MAPK pathway is another signal pathway closely related to PAH process, which is involved in PAH initiation and maintenance. It is not only associated with endothelial dysfunction and excessive cell proliferation, but also with RVH and RV dysfunction in PAH. In addition, MAPK can also induce inflammatory cascades and thus participate in PAH processes. MAPK can participate in the process of autophagy, leading to the degradation of macromolecules, apoptosis, and increased production of macrophage colony stimulating factor (GM-CSF), induce macrophage aggregation, and aggra-

vate PAH in human and experimental animals. In this experiment, MCT treatment for 6 weeks caused the up-regulation of p-ERK1/2 and p-P38 protein levels, indicating that MAPK is involved in the process of PAH and RVH, while sevofluran can regulate the expression of key MAPK proteins to reduce RV changes (**Figure 6**).

Limitation

We used a rat model of PAH induced by MCT intraperitoneal injection, a condition known to be characterized by increased inflammation, to assess the effects of sevoflurane. However, the animal model may have some differences from clinical patients with PAH, so more clinical studies may need to be performed to further identify whether cardioprotective properties of this volatile anesthetic are identical to what can be observed in animal model.

Evaluation of RV function is challenging. It can be directly assessed by right heart catheterization, which has a significant effect on the diagnosis, prognostic evaluation, and decision-making of PAH patients [34]. Clearly, RV catheterization with pressure-volume analyses would be valuable to better understand the load-independent parameter of RV function, like RV contractility and diastolic stiffness. And LV catheterization with pressure-volume analyses is helpful to understand how changes of RV affect the LV contractility. However, considering the pulmonary artery catheter is invasive and relative insecurity, and at the same time, it is not suitable for serially monitoring cardiac performance, we chose echocardiography to map the progression of cardiac dysfunction and structure changes. Studies had shown that it has obvious correlation with invasive hemodynamic examination and can replace catheterization [35, 36]. Novel technologies over the past 3 decades, such as speckle-tracking imaging-based regional LV analysis, perfusion imaging, fetal echocardiography, and myocardial deformation imaging etc., enable ultrasound echocardiography to be a powerful tool to translate small animals data to enhanced clinical understanding and treatment of cardiovascular diseases [37].

Conclusion

In this study, we demonstrated that reduced local inflammatory activity is associated with improved right heart function, absence of RVF, and reduced pulmonary vascular pathologic remodeling in experimental PAH. The beneficial effects of sevoflurane were associated with reduced IL-6 and TNF-α expressions and inhibition of NF-κB and MAPK. Our findings revealed cardioprotective properties of this volatile anesthetic and encourage further experimental and clinical investigations to study the molecular mechanism underlying this process.

Acknowledgements

Disclosure of conflict of interest

None.

Address correspondence to: Dr. Jiange Han, Department of Anesthesiology, Tianjin Chest Hospital, No. 261 South Taierzhuang Road, Tianjin 300222, China. Tel: +86-13821001156; E-mail: hanjiange@163.com; Dr. Jie Geng, Department of Cardiology, Tianjin Chest Hospital, No. 261 South Taierzhuang Road, Tianjin 300222, China. Tel: +86-022-8818-5157; E-mail: tjxk178@163.com

References

[1] Lucchinetti E, Lou PH, Gandhi M, Clanachan AS and Zaugg M. Differential effects of anesthetics and opioid receptor activation on cardioprotection elicited by reactive oxygen species-mediated postconditioning in sprague-dawley rat hearts. Anesth Analg 2018; 126: 1739-1746.

[2] Zhao YB, Zhao J, Zhang LJ, Shan RG, Sun ZZ, Wang K, Chen JQ and Mu JX. MicroRNA-370 protects against myocardial ischemia/reperfusion injury in mice following sevoflurane anesthetic preconditioning through PLIN5-dependent PPAR signaling pathway. Biomed Pharmacother 2019; 113: 108697.

[3] Guerrero Orriach JL, Galán Ortega M, Ramirez Fernandez A, Ramirez Aliaga M, Moreno Cortes MI, Ariza Villanueva D, Florez Vela A, Alcaide Torres J, Santiago Fernandez C, Matute Gonzalez E, Alsina Marcos E, Escalona Belmonte JJ, Rubio Navarro M, Garrido Sanchez L and Cruz Mañas J. Cardioprotective efficacy of sevoflurane vs. propofol during induction and/or maintenance in patients undergoing coronary artery revascularization surgery without pump: a randomized trial. Int J Cardiol 2017; 243: 73-80.

[4] Pagel PS and Crystal GJ. The discovery of myocardial preconditioning using volatile anesthetics: a history and contemporary clinical perspective. J Cardiothorac Vasc Anesth 2018; 32: 1112-1134.

[5] Uhlig C, Bluth T, Schwarz K, Deckert S, Heinrich L, De Hert S, Landoni G, Serpa Neto A, Schultz MJ, Pelosi P, Schmitt J and Gama de Abreu M. Effects of volatile anesthetics on mortality and postoperative pulmonary and other complications in patients undergoing surgery: a systematic review and meta-analysis. Anesthesiology 2016; 124: 1230-1245.

[6] Landoni G, Rodseth RN, Santini F, Ponschab M, Ruggeri L, Székely A, Pasero D, Augoustides JG, Del Sarto PA, Krzych LJ, Corcione A, Slullitel A, Cabrini L, Le Manach Y, Almeida RM, Bignami E, Biondi-Zoccai G, Bove T, Caramelli F, Cariello C, Carpanese A, Clarizia L, Comis M, Conte M, Covello RD, De Santis V, Feltracco P, Giordano G, Pittarello D, Gottin L, Guarracino F, Morelli A, Musu M, Pala G, Pasin L, Pezzoli I, Paternoster G, Remedi R, Roasio A, Zucchetti M, Petrini F, Finco G, Ranieri M and Zangrillo A. Randomized evidence for reduction of perioperative mortality. J Cardiothorac Vasc Anesth 2012; 26: 764-772.

[7] Landoni G, Pisano A, Lomivorotov V, Alvaro G, Hajjar L, Paternoster G, Nigro Neto C, Latronico N, Fominskiy E, Pasin L, Finco G, Lobreglio R, Azzolini ML, Buscaglia G, Castella A, Comis M, Conte A, Conte M, Corradi F, Dal Checco E, De Vuono G, Ganzaroli M, Garofalo E, Gazivoda G, Lembo R, Marianello D, Baiardo Redaelli M, Monaco F, Tarzia V, Mucchetti M, Belletti A, Mura P, Musu M, Pala G, Paltenghi M, Pasyuga V, Piras D, Riefolo C, Roasio A, Ruggeri L, Santini F, Székely A, Verniero L, Vezzani A, Zangrillo A and Bellomo R. Randomized evidence for reduction of perioperative mortality: an updated consensus process. J Cardiothorac Vasc Anesth 2017; 31: 719-730.

[8] Frustaci A, Petrosillo N, Vizza D, Francone M, Badagliacca R, Verardo R, Fedele F, Ippolito G and Chimenti C. Myocardial and microvascular inflammation/infection in patients with HIV-associated pulmonary artery hypertension. AIDS 2014; 28: 2541-2549.

[9] van der Baan A, Kortekaas KA, van Es E, Meier S, Klautz RJ and Engbers FH. Sevoflurane-enriched blood cardioplegia: the intramyocardial delivery of a volatile anesthetic. Perfusion 2015; 30: 295-301.

[10] Takai S, Jin D, Chen H, Li W, Yamamoto H, Yamanishi K, Miyazaki M, Higashino H, Yamanishi H and Okamura H. Chymase inhibition improves vascular dysfunction and survival in stroke-prone spontaneously hypertensive rats. J Hypertens 2014; 32: 1637-1648.

[11] D'Alonzo GE, Barst RJ, Ayres SM, Bergofsky EH, Brundage BH, Detre KM, Fishman AP, Goldring RM, Groves BM and Kernis JT. Survival in patients with primary pulmonary hypertension. Results from a national prospective registry. Ann Intern Med 1991; 115: 343-349.

[12] Wilson DW, Segall HJ, Pan LC and Dunston SK. Progressive inflammatory and structural changes in the pulmonary vasculature of monocrotaline-treated rats. Microvasc Res 1989; 38: 57-80.

[13] Ogoshi T, Tsutsui M, Kido T, Sakanashi M, Naito K, Oda K, Ishimoto H, Yamada S, Wang KY, Toyohira Y, Izumi H, Masuzaki H, Shimokawa H, Yanagihara N, Yatera K and Mukae H. Protective role of myelocytic nitric oxide synthases against hypoxic pulmonary hypertension in mice. Am J Respir Crit Care Med 2018; 198: 232-244.

[14] Tian W, Jiang X, Sung YK, Shuffle E, Wu TH, Kao PN, Tu AB, Dorfmüller P, Cao A, Wang L, Peng G, Kim Y, Zhang P, Chappell J, Pasupneti S, Dahms P, Maguire P, Chaib H, Zamanian R, Peters-Golden M, Snyder MP, Voelkel NF, Humbert M, Rabinovitch M and Nicolls MR. Phenotypically silent bone morphogenetic protein receptor 2 mutations predispose rats to inflammation-induced pulmonary arterial hypertension by enhancing the risk for neointimal transformation. Circulation 2019; 140: 1409-1425.

[15] Kurosawa R, Satoh K, Kikuchi N, Kikuchi H, Saigusa D, Al-Mamun ME, Siddique MAH, Omura J, Satoh T, Sunamura S, Nogi M, Numano K, Miyata S, Uruno A, Kano K, Matsumoto Y, Doi T, Aoki J, Oshima Y, Yamamoto M and Shimokawa H. Identification of celastramycin as a novel therapeutic agent for pulmonary arterial hypertension. Circ Res 2019; 125: 309-327.

[16] Savale L, Tu L, Rideau D, Izziki M, Maitre B, Adnot S and Eddahibi S. Impact of interleukin-6 on hypoxia-induced pulmonary hypertension and lung inflammation in mice. Respir Res 2009; 10: 6.

[17] Hudalla H, Michael Z, Christodoulou N, Willis GR, Fernandez-Gonzalez A, Filatava EJ, Dieffenbach P, Fredenburgh LE, Stearman RS, Geraci MW, Kourembanas S and Christou H. Carbonic anhydrase inhibition ameliorates inflammation and experimental pulmonary hypertension. Am J Respir Cell Mol Biol 2019; 61: 512-524.

[18] Sweatt AJ, Hedlin HK, Balasubramanian V, Hsi A, Blum LK, Robinson WH, Haddad F, Hickey PM, Condliffe R, Lawrie A, Nicolls MR, Rabinovitch M, Khatri P and Zamanian RT. Discovery of distinct immune phenotypes using machine learning in pulmonary arterial hypertension. Circ Res 2019; 124: 904-919.

[19] Cracowski JL, Chabot F, Labarère J, Faure P, Degano B, Schwebel C, Chaouat A, Reynaud-Gaubert M, Cracowski C, Sitbon O, Yaici A, Simonneau G and Humbert M. Proinflammatory cytokine levels are linked to death in pulmonary arterial hypertension. Eur Respir J 2014; 43: 915-917.

[20] Williams JL, Cavus O, Loccoh EC, Adelman S, Daugherty JC, Smith SA, Canan B, Janssen PML, Koenig S, Kline CF, Mohler PJ and Bradley EA. Defining the molecular signatures of human right heart failure. Life Sci 2018; 196: 118-126.

[21] Rohm I, Grün K, Müller LM, Bäz L, Förster M, Schrepper A, Kretzschmar D, Pistulli R, Yilmaz A, Bauer R, Jung C, Berndt A, Schulze PC and Franz M. Cellular inflammation in pulmonary hypertension: detailed analysis of lung and right ventricular tissue, circulating immune cells and effects of a dual endothelin receptor antagonist. Clin Hemorheol Microcirc 2019; 73: 497-522.

[22] Marra AM, Benjamin N, Cittadini A, Bossone E and Grünig E. When pulmonary hypertension complicates heart failure. Heart Fail Clin 2020; 16: 53-60.

[23] Zhang SB, Liu TJ, Pu GH, Li BY, Gao XZ and Han XL. Suppression of long non-coding RNA LINC00652 restores sevoflurane-induced cardioprotection against myocardial ischemia-reperfusion injury by targeting GLP-1R through the cAMP/PKA pathway in mice. Cell Physiol Biochem 2018; 49: 1476-1491.

[24] Qiao SG, Sun Y, Sun B, Wang A, Qiu J, Hong L, An JZ, Wang C and Zhang HL. Sevoflurane postconditioning protects against myocardial ischemia/reperfusion injury by restoring autophagic flux via an NO-dependent mechanism. Acta Pharmacol Sin 2019; 40: 35-45.

[25] Qian B, Yang Y, Yao Y, Liao Y and Lin Y. Upregulation of vascular endothelial growth factor receptor-1 contributes to sevoflurane preconditioning-mediated cardioprotection. Drug Des Devel Ther 2018; 12: 769-776.

[26] Wu J, Yang L, Xie P, Yu J, Yu T, Wang H, Maimaitili Y, Wang J, Ma H, Yang Y and Zheng H. Cobalt chloride upregulates impaired HIF-1α expression to restore sevoflurane post-conditioning-dependent myocardial protection in diabetic rats. Front Physiol 2017; 8: 395.

[27] Xue QS, Luo Y and Zhang FJ. Expert concensus on the clinical practice of inhalation anesthesia (quick). China Continuing Medical Education 2011; 3: 108-112.

[28] Tang QF, Fang ZY and Shi CH. The protective effect and mechanism of sevoflurane on LPS-induced acute lung injury in mice. Am J Transl Res 2017; 9: 1732-1742.

[29] Du G, Wang S, Li Z and Liu J. Sevoflurane post-treatment attenuates lung injury induced by oleic acid in dogs. Anesth Analg 2017; 124: 1555-1563.

[30] Araújo MN, Santos CL, Samary CS, Heil LBB, Cavalcanti VCM, Cruz FF, Felix NS, Silva JD, Morales MM, Pelosi P, Fernandes FC, Villela NR, Silva PL and Rocco PRM. Sevoflurane, compared with isoflurane, minimizes lung damage in pulmonary but not in extrapulmonary acute respiratory distress syndrome in rats. Anesth Analg 2017; 125: 491-498.

[31] Kellner P, Müller M, Piegeler T, Eugster P, Booy C, Schläpfer M and Beck-Schimmer B. Sevoflurane abolishes oxygenation impairment in a long-term rat model of acute lung injury. Anesth Analg 2017; 124: 194-203.

[32] Jabaudon M, Boucher P, Imhoff E, Chabanne R, Faure JS, Roszyk L, Thibault S, Blondonnet R, Clairefond G, Guérin R, Perbet S, Cayot S, Godet T, Pereira B, Sapin V, Bazin JE, Futier E and Constantin JM. Sevoflurane for sedation in acute respiratory distress syndrome. A randomized controlled pilot study. Am J Respir Crit Care Med 2017; 195: 792-800.

[33] Wu Q, Wu W, Jacevic V, Franca TCC, Wang X and Kuca K. Selective inhibitors for JNK signalling: a potential targeted therapy in cancer. J Enzyme Inhib Med Chem 2020; 35: 574-583.

[34] Kubiak GM, Ciarka A, Biniecka M and Ceranowicz P. Right heart catheterization-background, physiological basics, and clinical implications. J Clin Med 2019; 8: 1331.

[35] Watson LE, Sheth M, Denyer RF and Dostal DE. Baseline echocardiographic values for adult male rats. J Am Soc Echocardiogr 2004; 17: 161-167.

[36] Prakash R and Lindsay P. Determination of right ventricular wall thickness by echocardiogram. JAMA 1978; 239: 638-640.

[37] Wang LW, Kesteven SH, Huttner IG, Feneley MP and Fatkin D. High-frequency echocardiography-transformative clinical and research applications in humans, Mice, and Zebrafish. Circ J 2018; 82: 620-628.